TÜBİTAK

Research Article

Turk J Agric For
35 (2011) 579-589
© TÜBİTAK
doi:10.3906/tar-1003-826

Mapping paddy rice yield in Zhejiang Province using MODIS spectral index

Qian CHENG*, Xiuju WU

Department of Environmental Resources Management and City Planning, Zhejiang Gongshang University, Hangzhou, 310035 - CHINA

Received: 21.03.2010

Abstract: The first 19 bands of a moderate-resolution imaging spectrometer (MODIS), covering the visible to shortwave infrared spectral wavelength, were simulated by ground-level reflectance spectra. All spectral indices similar to the normalized difference vegetation index (NDVI) and ratio vegetation index (RVI) formed by every 2 bands were calculated to obtain their determination coefficients, with theoretical and real yield. Results revealed that the combinative near-infrared (NIR) index (band 2 and band 19, symbol b2 and b19, and other similar ones) and the (b16, b19) of MODIS were strongly correlated with rice yield, especially the correlative coefficient that exceeded significant levels in the maturing stage. However, combinative visible light index was correlated with rice yield strongly in the early stage and poorly in the latter stage. The best spectral indices for predicting rice yield in whole rice growth were the combinations of (b2, b19) and (b16, b19). Based on the 2-band combination of the (b2, b19) of MODIS and the constructed estimating model, the rice yield of Zhejiang Province was estimated and its spatial distribution was mapped. Estimated results based on MODIS images were validated using 8 measured validation sites. Errors in the estimated rice yield ranged from 3.2% to 20.3%, with a mean value of 10.1%. The results indicated that the 2-band combination of the (b2, b19) MODIS index was most suitable for monitoring rice yield.

Key words: Estimation, rice yield, MODIS, spectral index

Introduction

Among the various modern methods for estimating rice yield, remote sensing is of primary importance. This is a result of its capability to provide synoptic information over wide areas with high acquisition frequency. Remote sensing techniques have been employed to estimate various plant parameters (Wiegant et al. 1979; Price 1995; Mirik et al. 2007) and crop yield (Cheng 2004; Cheng 2006). Remote sensing provides quantitative information on agricultural crops instantaneously and nondestructively (Clevers 1988; Mirik et al. 2006), and the spatial and temporal distributions of crop production offer valuable information for agricultural management and biogeochemical modeling efforts (Lobell et al. 2003; Sonmez and Sari 2006).

Many vegetation indices have been developed and applied in vegetation studies since the first vegetation index, the ratio vegetation index (RVI) (Jordan 1969; Broge and Leblanc 2000). Vegetation indices may employ simple ratios of any 2 single wavelength combinations. These ratios were found to be fairly effective in normalizing the effect of reflectance variation in soil background (Colwell 1973).

* E-mail: qiancheng525@163.com

The originally normalized difference vegetation index (NDVI), discussed by Rouse et al. (1973), is an effective vegetation measure since it is sufficiently stable to permit meaningful comparisons between seasonal and interannual changes in vegetation growth and activity. This is because it can reduce different forms of multiplicative noise (illumination differences, cloud shadows, atmospheric attenuation, and certain topographic variations) present in multiple bands (Myneni et al. 1995). Many models for simulating rice growth using vegetation indices have been developed, such as SIMRIW (Horie et al. 1992), RICAM (Yin and Qi 1994), and a rice-weed competition model (Graf et al. 1990). Using 16 years of NOAA AVHRR satellite data (collected between 1987 and 2002) (Wall et al. 2008), the NDVI was employed to model weekly wheat yield in 40 census agricultural regions (CAR) in the Canadian prairies throughout the entire growing season. The simulated broad-band NDVI and narrow-band NDVI-type indices, which include all possible 2-band combinations of the 102 bands in the hyperspectral imagery, were calculated and related to yield.

Meanwhile, an enhanced vegetation index (EVI) was developed to improve sensitivity over high biomass regions and vegetation monitoring capabilities by decoupling the canopy background signal and reducing atmospheric influences (Liu and Huete 1995). The RVI, NDVI, enhanced vegetation index (EVI), wide dynamic range vegetation index (WDRVI), and several hyperspectral reflectance indices were used to estimate crop yield (Dalezios et al. 2001; Wong et al. 2006; Zhao et al. 2007), and the ability of various vegetative indices (VIs) were evaluated to detect canopy architectures in wheat genotypes (Zhao et al. 2009).

Spectral data from the current generation of earth-orbiting satellites carrying broadband sensors, such as Landsat TM and NOAA/AVHRR, are saddled by limitations in providing accurate estimates of crop yield (Thenkabail et al. 1995; Fassnacht et al. 1997). These limitations have motivated the inclusion of hyperspectral sensors onboard the new generation of satellites planned by various governments and the private sector in the United States. The upcoming narrow-band hyperspectral sensors include the following: 1) Hyperion sensor with 220 spectral bands, each with narrow bands 10 nm in width, onboard the Earth Observer-1 (EO-1) of the National Atmospheric and Space Administration's (NASA) New Millennium Program; 2) hyperspectral imaging spectrometer sensor with 105 spectral bands onboard the Australian Resource Information Environmental Satellite-1; 3) moderate resolution imaging spectrometer (MODIS) with 36 channels, onboard Terra (Running et al. 1999).

The MODIS aboard the Terra (EOS AM) and Aqua (EOS PM) satellites improves the performance of AVHRR by providing higher spatial and spectral resolution, enabling more detailed analyses of earth systems. MODIS products are designed to provide consistent spatial and temporal comparisons between different global vegetation conditions that can be used to monitor photosynthetic activity and forecast crop yields (Vazifedoust et al. 2009). MODIS-NDVI data, with 250-m resolution, was used to estimate the winter wheat yield in one of the main winter wheat growing regions (Ren et al. 2008).

Rice is by far the most important genus of Chinese crops. Only a few studies in the past have dealt with the relationship between the combinative bands of simulated MODIS bands and rice yield. Therefore, the objective of this study was to establish relationships between simulated MODIS bands and rice yield, determine the suitable index for estimating rice yield, map the rice yield of Zhejiang Province based on the suitable index and MODIS image, and validate Zhejiang Province's rice yield based on ground-measured data.

Materials and methods

Experimental field description

The experiment was conducted in a paddy field at the Zhejiang University experimental farm in Hangzhou, China (30°14′N, 120°10′E) in 2002 and 2003. Mean annual precipitation is 1320.9 mm and mean annual temperature is 16.2 °C. The experimental field contains paddy soil, sandy loam in texture, with the following properties: available N, 188.5 mg kg^{-1}; available P, 34.8 mg kg^{-1}; available K, 72.7 mg kg^{-1}; organic matter, 9.96 g kg^{-1}; and pH, 6.78. Measuring methods were based on those of Bao (2005).

Single plants were transplanted at a spacing of 0.13 by 0.17 m in 24 randomly chosen plots for every 4.76 × 4.68 m. The plots were composed of 2 cultivars and 3 nitrogen levels (0, 120, and 240 kg N ha^{-1}) with 4 replications. The 3 treatment levels represented: no nitrogen fertilizer, a proper application, and a superabundant dose. Furthermore, 533.3 kg $Ca(H_2PO_4)_2$ ha^{-1} was applied as a base fertilizer and 300 kg KCl ha^{-1} as a heading fertilizer.

Rice cultivars Xiushui 110 (commonly known as japonica rice, with a growing period of approximately 145 days) and Xieyou 9308 (hybrid indica rice, with a growing period of approximately 140 days) were selected for investigation. These were seeded on 2 June 2002 and 3 June 2003 and transplanted on 25 June 2002 and 27 June 2003. Growth of Xiushui 110 was observed on 2 September 2002 and 5 September 2003, while growth of Xieyou 9308 was recorded on 30 August 2002 and 29 August 2003.

Validating sample sites

Another validating sample site, the town of Yuhang, is located 40 km west of Hangzhou in Zhejiang Province, China. It measures approximately 10 km^2, its upper left district is situated at 30°30′N, 119°15′E, and its lower right district is situated at 30°10′N, 120°15′E (Figure 1). Fieldwork was conducted during a single rice growing season, from June to November 2002. Positions for all selected measurement points were recorded using a Magellan ProMark X global positioning system (GPS).

On 24 July, 2 September, 8 October, and 4 November 2002, 4 field campaigns were conducted at the Yuhang study field. Each sampling site measured 100 × 100 m, with 5 observation points (A1, A2, A3, A4, and A5) measuring 1 × 1 m in each sample plot (Figure 2).

Spectral reflectance measurement

An ASD FieldSpec Pro FR spectral radiometer (Analytical Spectral Devices, Boulder, Colorado) with a range of 350-2500 nm was used. It had a spectral sampling interval of 1.4 and resolution of 3 nm for the 350-1000 nm range, and a sampling interval of 2 and resolution of 10 nm for the 1000-2500 nm range. Canopy spectral reflectance was determined on sunny days without clouds or wind at the heading, milking, and maturing stages of rice cultivation. The detector was placed approximately 0.70 m above the canopy. A sampling spectrum consisted of 10 readings, with 10 sampling spectra averaged to represent the canopy mean spectral reflectance. Dark signals were subtracted and spectral data were compared to those of a standard white reference as spectral measurement.

MODIS image acquirement

According to the farming practice in the study area, MOD09, covering the whole of Zhejiang Province, was acquired on 25 October 2002 with the support of NASA. The date corresponded with the late rice planting season. The software packages employed for image and geoinformation analyses were ENVI 3.4 and ARC/INFO 8.1. Topographic maps, land maps with 1:250,000 scales, recently produced maps of vegetation types, land cover and land use maps, and other ancillary geoinformation were used in the study, as well. GPS was tapped to register the training samples.

Theoretical and real yield acquirement

When the rice matured, efficient spikes at each sample socket from every plot were measured and average effective grain numbers were determined. Real yield at every plot was weighted. Theoretical and real yields were calculated using the following formulas.

Theoretical yield unit area = (efficient spikes every socket × effective grain numbers × 1000-grain weight × whole socket)/1000

Real yield unit area = real yield of plot/plot area

Methodology

Various vegetation indices have been developed for qualitative and quantitative assessment of vegetation using remote spectral measurements (Bannari et al. 1995). Specifically, sensors with spectral bands in the red (RED) and near-infrared (NIR) are effective in vegetation monitoring, as the difference between them has been deemed a strong indicator of the amount of photosynthetically active green biomass (Tucker 1979). As a result, there is widespread use of the NDVI and RVI.

In this paper, field-measured hyperspectral data with ranges from 350 to 2500 nm were employed to simulate the reflectance of the first 19 bands of MODIS (Table 1).

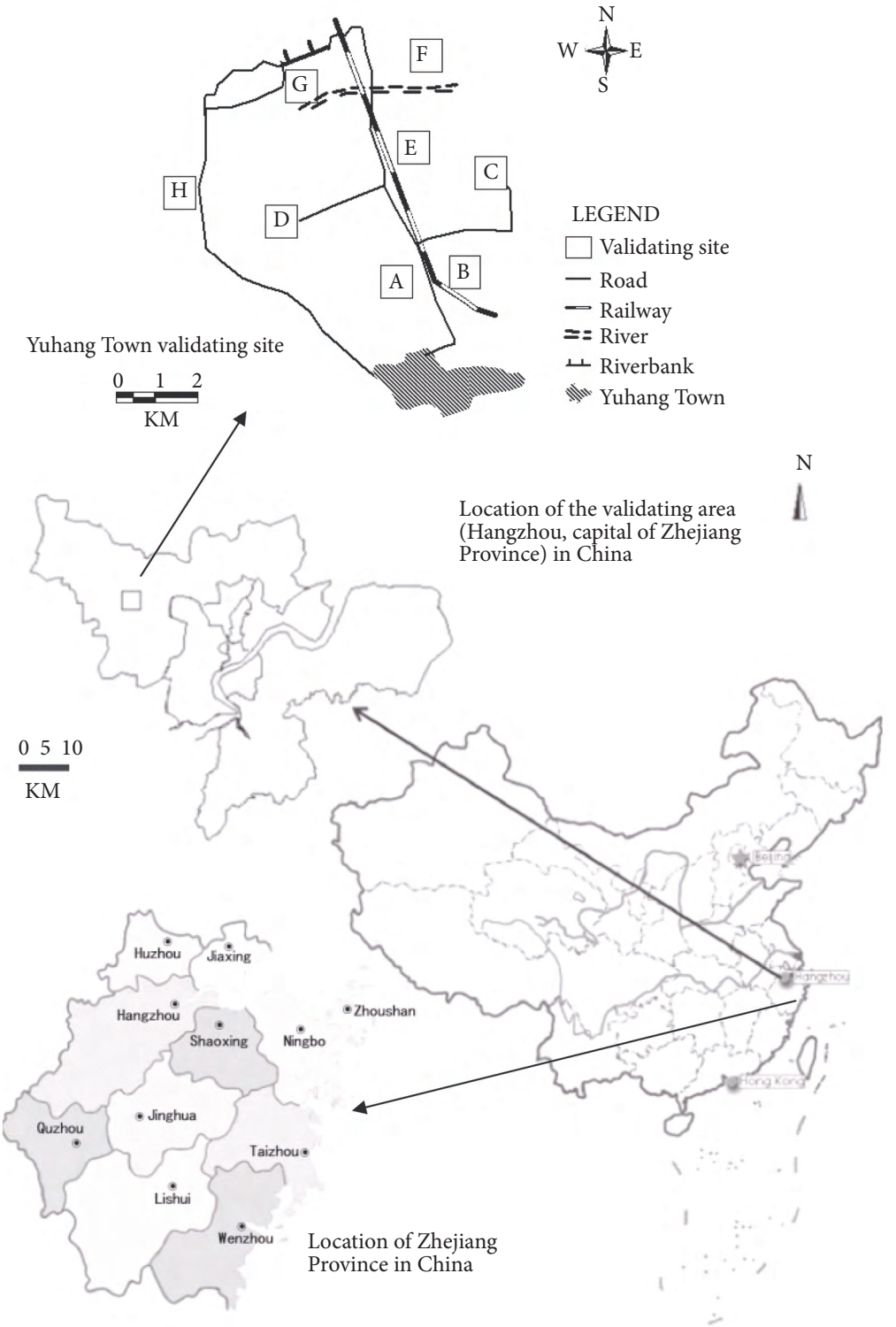

Figure 1. Location of the validating site in Hangzhou, distribution of the different validating sample plots in Yuhang Town, and location of the study area (Zhejiang Province) in China (A, B, C, D, E, F, G, and H represent the validating sample sites).

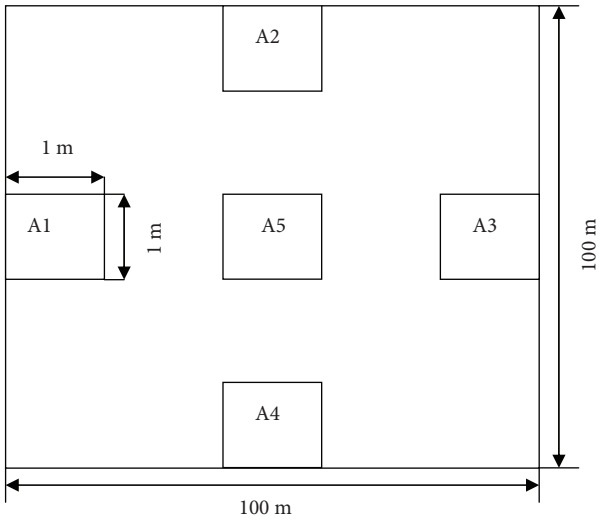

Figure 2. Location of the sample points in the validating sample plot (A1, A2, A3, A4, and A5 represent the observation points).

Table 1. Bandwidth ranges of MODIS for bands 1-19.

Band	Bandwidth ranges (μm)	Band	Bandwidth ranges (μm)	Band	Bandwidth ranges (μm)
1	0.620-0.670	8	0.405-0.420	14	0.673-0.683
2	0.841-0.876	9	0.438-0.448	15	0.743-0.753
3	0.459-0.479	10	0.483-0.493	16	0.862-0.877
4	0.545-0.565	11	0.526-0.536	17	0.890-0.920
5	1.230-1.250	12	0.546-0.566	18	0.931-0.941
6	1.628-1.652	13	0.662-0.672	19	0.915-0.965
7	2.105-2.155				

The following equation was used to simulate MODIS bands:

$$R_i = \frac{\sum_{j=l}^{n} r_{\lambda_j}}{n} \quad (1)$$

where R and r pertain to the reflectance of MODIS and ground spectral, i is the band name of MODIS, λ_1 and λ_n are the beginning and ending bands of MODIS, and n is the band numbers between λ_1 and λ_n.

NDVI, RVI, and EVI were calculated using the following formulas:

$$NDVI(bj, bi) = (R_{bj} - R_{bi}) / (R_{bj} + R_{bi}) \quad (2)$$

$$RVI(bj, bi) = R_j / R_i \quad (3)$$

where bi and bj are the ith and jth bands and R is the reflectance.

$$EVI = (1 + L)\frac{R_{NIR} - R_{Red}}{R_{NIR} + C_1 R_{Red} - C_2 R_{Blue} + L} \quad (4)$$

where,, and are the surface reflectance for the respective MODIS bands; L is a canopy background calibration factor that normalizes differential RED and NIR extinction through the canopy; and C_1 and C_2 are the weighing factors for the aerosol resistance. The coefficients adopted in the EVI algorithm were L = 1, C_1 = 6, and C_2 = 7.5.

Results

The best combination index of MODIS for monitoring rice yield

C^2_{19} combinations of NDVI and RVI spectral indices of the simulated first 19 bands of MODIS were acquired after 2 bands were formed, and the coefficient between the NDVI and RVI spectral indices was determined. The result of this comprehensive analysis is illustrated in contour plots of the R^2 values in the maturing stage in Figures 3 and 4.

Results revealed that the determination coefficient R^2 of NDVI combinations (b2, b19) and (b16, b19), in theoretical and real yields, was highly significant for 3 growing stages, reaching the highest in the maturing stage with R^2 = 0.74. The determination coefficient R^2 of combinations (b17, b19) and (b16, b17) was high in the maturing stage, but lower in other growing stages. On the other hand, the determination coefficient R^2 of combinations (b1, b14), (b1, b13), (b8, b11), and (b9, b11) was the highest in the heading stage and did not exceed the significant level in the maturing stage. Table 2 illustrates the determination coefficient R^2 of the MODIS spectral index in the 3 growing stages, with theoretical and real yields. Table 2 shows that the determination coefficient R^2 between EVI, combinations of (b2, b19) and (b16, b19), and rice yield in the whole stage was high, exceeding the extremely significant level. Meanwhile, the determination coefficient R^2 between the NDVI of combination (b1, b2) was low, not exceeding the significant level. The combination of NDVI and RVI was superior to EVI in monitoring rice yield in the middle and late stages. From Table 2, the best indices are seen to be the NDVI combinations of (b2, b19), (b16, b19), and EVI.

Corresponding data in the field obtained in 2003 was applied to validate the accuracy of theoretical yield models of combinative EVI and NIR band combination. The accuracy of the model for the band combination (b2, b19) was 92.1%, the accuracy of (16, 19) was 91.9%, and the accuracy of EVI was 87.2% in the maturing stage (Table 3).

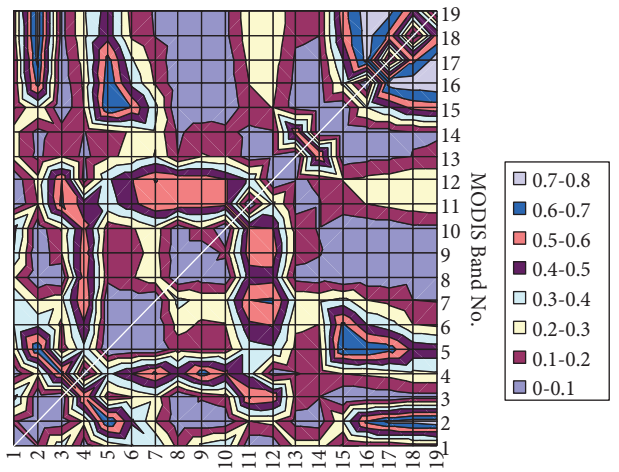

Figure 3. Plot of the determination coefficient between MODIS-NDVI and the theoretical and real yields (theoretical yield above the diagonal, real yield below the diagonal) (3 October 2002).

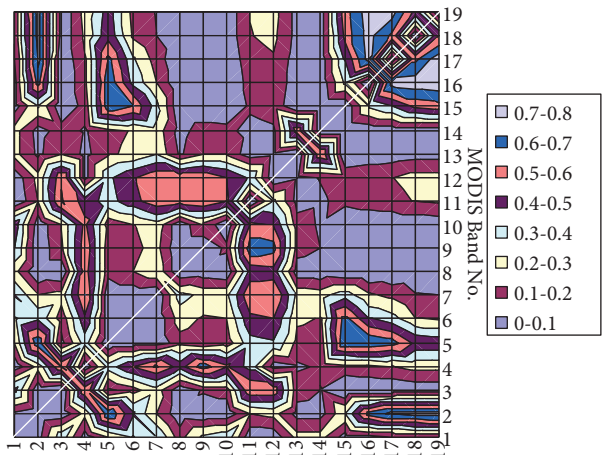

Figure 4. Plot of the determination coefficient between MODIS-RVI and the theoretical and real yields for rice (theoretical yield above the diagonal, real yield below the diagonal) (3 October 2002).

Table 2. The better combinations of NDVI and RVI and their corresponding determination coefficients for the 3 growth stages of rice.

Heading stage (HS) (31 August 2002)								
NDVI	(b2, b19)	(b16, b19)	(b3, b11)	(b8, b11)	(b9, b11)	(b1, b14)	(b1, b13)	(b1, b2)
TY	0.2696	0.2977	0.7212	0.7362	0.7470	0.8138	0.7672	0.2528
RY	0.2488	0.2463	0.7626	0.7417	0.7673	0.8047	0.7856	0.1877
RVI	(b2, b19)	(b16, b19)	(b3, b11)	(b8, b11)	(b9, b11)	(b1, b14)	(b1, b13)	(b1, b2)
TY	0.2725	0.2645	0.6981	0.7133	0.7216	0.8148	0.7696	0.2315
RY	0.2520	0.2495	0.7505	0.7374	0.7559	0.8012	0.7841	0.1585
Milking stage (MIS) (20 September 2002)								
NDVI	(b2, b19)	(b16, b19)	(b3, b11)	(b3, b12)	(b3, b4)	(b1, b14)	(b1, b13)	(b1, b2)
TY	0.3573	0.3805	0.6989	0.6804	0.6876	0.6754	0.645	0.0029
RY	0.3082	0.3284	0.6726	0.6492	0.6495	0.6816	0.6614	0.0124
RVI	(b2, b19)	(b16, b19)	(b3, b11)	(b8, b11)	(b9, b11)	(b1, b14)	(b1, b13)	(b1, b2)
TY	0.3652	0.3881	0.7021	0.6826	0.6886	0.6716	0.6398	0.0184
RY	0.3148	0.3348	0.6732	0.6489	0.6486	0.6792	0.6574	0.0260
Maturing stage (MAS) (3 October 2002)								
NDVI	(b2, b19)	(b16, b19)	(b17, b19)	(b16, b17)	(b2, b17)	(b2, b18)	(b16, b18)	(b1, b2)
TY	0.7494	0.7502	0.7377	0.7283	0.7246	0.7374	0.7372	0.1184
RY	0.7657	0.7688	0.7606	0.7357	0.7271	0.7511	0.7531	0.1074
RVI	(b2, b19)	(b16, b19)	(b17, b19)	(b16, b17)	(b2, b17)	(b2, b18)	(b16, b18)	(b1, b2)
TY	0.7565	0.7568	0.7435	0.7288	0.7256	0.7426	0.7417	0.0689
RY	0.7719	0.7746	0.7659	0.7360	0.7277	0.7555	0.7571	0.0659

HS	TY	RY	MIS	TY	RY	MAS	TY	RY
EVI	0.3349	0.3817	EVI	0.5633	0.4622	EVI	0.4955	0.5866

TY: theoretical rice yield, RY: real rice yield

Table 3. The spectral index estimation models of theoretical rice yield (kg ha^{-1}) and estimation accuracy.

Band combination	Heading stage (31 August 2002)			Milking stage (20 September 2002)			Maturing stage (3 October 2002)		
	Estimation model	R^2	A (%)	Estimation model	R^2	A (%)	Estimation model	R^2	A (%)
EVI	y = 6772.7x + 5074.4	0.3349	85.0	y = 15864x + 1953.4	0.5633	86.3	y = 12987x + 4063.7	0.4955	87.2
Band (1, 2)	y = 15958x – 5657	0.2528	55.1	y = - 1250.1x + 10012	0.0029	35.5	y = 7462.1x + 3193.9	0.1184	32.7
Band (2, 19)	y = 53154x + 9977	0.2696	67.4	y = 94297x + 11642	0.3573	85.7	y = 73214x + 10464	0.7494	92.1
Band (16, 19)	y = 53424x + 10077	0.2977	67.4	y = 102338x + 12067	0.3805	78.3	y = 77552x + 10737	0.7502	91.9

y: rice yield, x: spectral index of band combination, A: estimation accuracy

Rice yield estimation of Zhejiang Province based on MODIS image

Based on the above analysis (Table 2), the combinative index (b2, b19) of MODIS has a better correlation coefficient than the combinative NIR index (b16, b19) in rice yield. Thus, the best index of combination (b2, b19) and MOD09 on 25 October 2002 were selected and applied in the following model:

$$Y = 73214X + 10464, \qquad R^2 = 0.75, \qquad (5)$$

where Y is the rice yield and X is the combinative index (b2, b19).

The rice yield of Zhejiang Province was estimated. Spatial distribution of rice on a large scale was determined by environmental factors such as climate, soil, moisture, and soil properties, as well as economic factors such as agricultural technology and historical culture. Paddy land and dry farming land in China possess significant differences in terms of suitability to the geographical background. This may be characterized by their spatial distribution along the environmental zone.

Spatial distribution of Zhejiang Province's rice yield, inferred for 2002, is presented in Figure 5. Yield varies according to the variety of rice as well as the soil type/topography in areas where this agricultural plant is cultivated. The images are presented in color scale. The dark green areas represent regions where the model provides high values. White or bright pixels represent areas with lower-yield values, while the variation of bright pixels indicates variation in rice yield.

Rice yields in the Huzhou, Jiaxing, and Jinghua regions are higher, while yields in the Hangzhou and Lishui regions are lower. The rice yield shown in Figure 5 provides valuable information for land-use assessments and MODIS efforts. For example, different regions can be matched with different tillage, fertilizer, and irrigation practices, providing the spatial constraints on management practices needed in biogeochemical models.

Validation of Zhejiang Province's rice yield based on ground-measured data

Estimation of rice yield for all sampling sites was performed based on the MODIS combinations of (b2, b19). Over the study site, 2 sets of nearly simultaneous in situ and satellite measurements were acquired using field measurement and MODIS. Ground data was geolocated with the coarser MODIS data.

Sample sites, located using GPS, were mapped to a georeferenced MODIS image from 25 October 2002. This resulted in a total of 8 pairs of rice yields. The mean of 5 measured rice yield points in the sample plot corresponded to 1 pixel of rice yield mapped, based on MODIS.

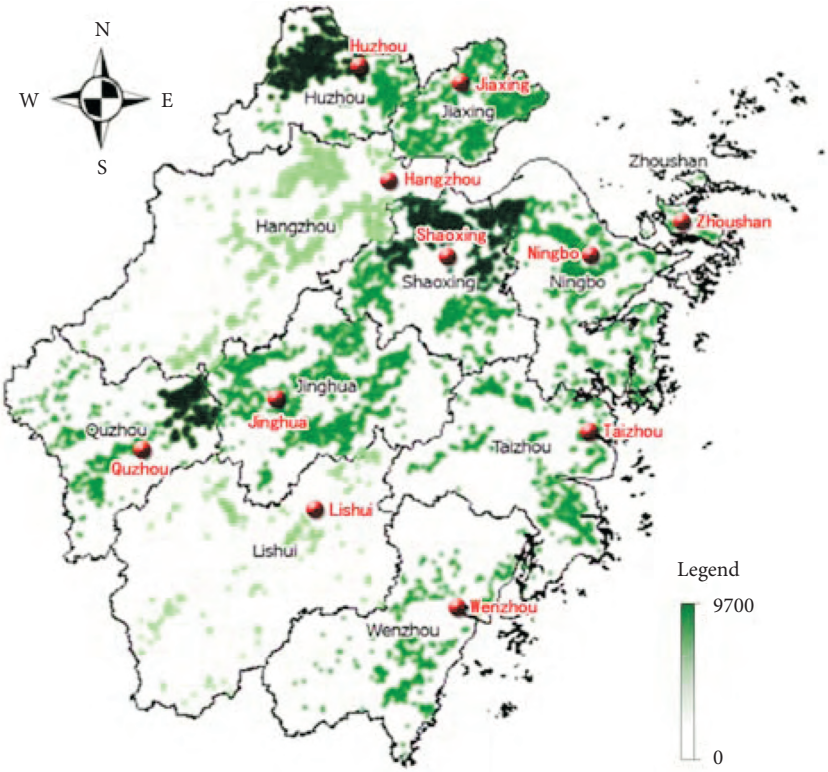

Figure 5. The 2002 distribution of rice yield (kg ha^{-1}) of Zhejiang Province based on MODIS image.

Estimated results were validated using 8 validation sites in the Yuhang area of Zhejiang Province (Figures 1 and 2). The results presented in Table 4 indicate that the estimated rice yield was spatially variable among the sampling sites, ranging from 7953.6 kg ha^{-1} to 9545.4 kg ha^{-1}, with a mean of 8625.2 kg ha^{-1} and RMSE of 924.7 kg ha^{-1}. Errors in the estimated rice yield ranged from 3.2% to 20.3%, with a mean value of 10.1%.

Discussion

In this experiment, rice canopy spectral data in the heading, milking, and maturing stages, as well as theoretical and real yields of plot, were measured. The first 19 bands of MODIS were simulated. The relationships between NDVI and RVI, based on 2-band combination and theoretical and real yields, were analyzed.

It is sufficient to display only the matrix below (or above) the diagonal matrix, as the R^2 (b1, b2) values are symmetrical. Similar contour plots (too numerous to be presented in this study) were created for all other growing stages. The b1, b8, b9, b11, b13, and b14 symbols are situated in the visible light region, while b2, b16, and b19 are situated in the NIR-infrared region. This is because, in the heading stage, visible light can effectively reflect sizeable variation in chlorophyll. Thus, the visible light bands were strongly correlated with rice yield at the beginning of the growing stage. With the growth of rice, especially in the maturing stage, pigments have a limited effect on the canopy spectra with yellow leaf, and NIR is strongly correlated with rice yield through reflecting of the rice colony. Rice yield was higher with better rice growth, and spectral reflectance in the NIR region was higher. Thus, combinative MODIS spectral index in the NIR region can effectively monitor rice yield, and this concurs with a number of earlier investigations (Liu et al. 2004; Tang et al. 2004).

Table 4. Rice yield estimated by MODIS index of combination (b2, b19), with means and standard deviations for each date, as well as related errors.

Site	A	B	C	D	E	F	G	H		
Lat.	30.290	30.303	30.311	30.305	30.315	30.290	30.311	30.315		
Lon.	119.93	119.93	119.94	119.91	119.92	119.93	119.94	119.92		
	Estimated rice yield (kg ha^{-1})								Mean	RMSE[a]
Yield (estimated)	8245.7	7953.6	8949.9	8280.4	8588.5	8438.5	9545.4	8999.4	8625.2	924.7
Yield (measured)	7883.2	7707.2	7888.3	7949.3	7665.8	7954.3	7938.1	7679.1	7833.2	
Error (%)	4.6	3.2	13.5	4.2	12.0	6.1	20.3	17.2	10.1	

[a]RMSE: root mean squared error

Results revealed that combinative NIR indices (b2, b19) and (b16, b19) of MODIS were strongly correlated with rice yield, especially the correlative coefficient, which exceeded the significant level in the maturing stage. However, combinative visible light indices (b1, b13), (b1, b14), (b9, b11), and (b8, b11) were strongly correlated with rice yield in the early stage and poorly correlated in the late stage.

The rice yield of Zhejiang Province, based on MODIS, was estimated. The spatial distribution of the rice yield of Zhejiang Province was mapped based on the 2-band combination of (b2, b19) of MODIS. Estimated results based on MODIS images were validated using 8 measured validation sites, and the errors in estimated rice yield ranged from 3.2% to 20.3%, with a mean value of 10.1%.

Results of the best index of combinations of (b2, b19) analysis revealed several interesting properties of yield estimates. Yield assessments were primarily sensitive to the method employed for computing NDVI. The most accurate estimates resulted from NDVI, supporting the combined use of (b2, b19) measurements. Results indicated that the 2-band combination of the (b2, b19) index of MODIS was most suitable for monitoring rice yield.

Acknowledgements

We appreciate the constructive suggestions of all anonymous reviewers. This work was supported by the Zhejiang Natural Science Foundation of China (Y5080071) and by the Plan of Star and Fire of the Ministry of Science and Technology of China (2008GA700061).

References

Bannari A, Morin D, Bonn F, Huete AR (1995) A review of vegetation indices. Remote Sensing Review 13: 95-120.

Bao SD (2005) Chemical and Agricultural Analysis of Soil. China Agriculture Press, Beijing, China.

Broge NH, Leblanc E (2000) Comparing prediction power and stability of broadband and hyperspectral vegetation indices for estimation of green leaf area index and canopy chlorophyll density. Remote Sensing of Environment 76: 156-172.

Cheng Q (2006) Multisensor comparisons for validation of MODIS vegetation indices. Pedosphere 16: 362-370.

Cheng Q, Huang JF, Wang RC (2004) Assessment of rice fields by GIS/GPS-supported classification of MODIS data. Journal of Zhejiang University (SCIENCE) 5: 412-417.

Clevers JG (1988) The derivation of a simplified reflectance model for the estimation of leaf area index. Remote Sensing of Environment 25: 53-69.

Colwell JE (1973) Bidirectional Spectral Reflectance of Grass Canopies for Determination of Above Ground Standing Biomass. PhD Thesis. University of Michigan, Michigan, USA.

Dalezios NR, Domenikiotis C, Loukas A, Tzortzios ST, Kalaitzidis C (2001) Cotton yield estimation based on NOAA/AVHRR produced NDVI. Physics and Chemistry of the Earth (B) 26: 247-251.

Fassnacht KS, Gower ST, Mackenzie MD, Nordheim EV, Lillesand TM (1997) Estimating the leaf area index of north central Wisconsin forests using the Landsat Thematic Mapper. Remote Sensing of Environment 61: 229-245.

Graf B, Rakotobe O, Zahner P, Delucchi V, Gutierrez AP (1990) A simulation model for the dynamics of rice growth and development: Part I - the carbon balance. Agricultural Systems 32: 341-365.

Horie T, Yajima M, Nakagawa H (1992) Yield forecasting. Agricultural Systems 40: 211-236.

Jordan CF (1969) Derivation of leaf area index from quality of light on the forest floor. Ecology 50: 663-666.

Liu H, Huete AR (1995) A feedback based modification of the NDVI to minimize canopy background and atmospheric noise. IEEE Transactions on Geoscience and Remote Sensing 33: 457-465.

Liu LY, Wang JH, Huang WJ (2004) Improving winter wheat yield prediction by novel spectral index. Transactions of the CSAE 20: 172-175 (in Chinese).

Lobell DB, Asner GP, Ortiz-Monasterio JI, Benning TL (2003) Remote sensing of regional crop production in the Yaqui Valley, Mexico: estimates and uncertainties. Agriculture, Ecosystems and Environment 94: 205-220.

Mirik M, Michels GJ, Kassymzhanova Mirik S, Elliott NC, Catana V (2006) Spectral sensing of aphid (Hemiptera: Aphididae) density using field spectrometry and radiometry. Turkish Journal of Agriculture and Forestry 30: 421-428.

Mirik M, Norland JE, Biondini ME, Crabtree RL, Michels GJ (2007) Relationships between remotely sensed data and biomass components in a big sagebrush (*Artemisia tridentata*) dominated area in Yellowstone National Park. Turkish Journal of Agriculture and Forestry 31: 135-145.

Myneni RB, Hall FG, Sellers PJ, Marshack AL (1995) The interpretation of spectral vegetation indices. IEEE Transactions on Geoscience and Remote Sensing 33: 481-486.

Price JC, Bausch WC (1995) Leaf area index estimation from visible and NIR-infrared reflectance data. Remote Sensing of Environment 52: 55-65.

Ren JQ, Chen ZX, Zhou QB, Tang HJ (2008) Regional yield estimation for winter wheat with MODIS-NDVI data in Shandong, China. International Journal of Applied Earth Observation and Geoinformation 10: 403-413.

Rouse JW, Haas RH, Schell JA, Deering DW (1973) Monitoring vegetation systems in the Great Plains with ERTS. Proceeding of 3rd ERTS Symposium, pp. 48-62.

Running SW, Baldocchi DD, Turner DP, Gower ST, Bakwin PS, Hibbard KA (1999) A global terrestrial monitoring network integrating tower fluxes, flask sampling, ecosystem modeling and EOS satellite data. Remote Sensing of Environment 70: 108-127.

Sönmez NK, Sarı M (2006) Use of remote sensing and geographic information system technologies for developing greenhouse databases. Turkish Journal of Agriculture and Forestry 30: 413-420.

Tang YL, Huang JF, Wang RC (2004) Comparison of yield estimated models of rice by remote sensing. Transactions of the CSAE 20: 166-171 (in Chinese).

Thenkabail PS, Ward AD, Lyon JG (1995) Landsat-5 Thematic Mapper models of soybean and corn crop characteristics. International Journal of Remote Sensing 15: 49-61.

Tucker CJ (1979) Red and photographic infrared linear combinations for monitoring vegetation. Remote Sensing of Environment 8: 127-150.

Vazifedoust M, Van Dam JC, Bastiaanssen W, Feddes R (2009) Assimilation of satellite data into agrohydrological models to improve crop yield forecasts. International Journal of Remote Sensing 30: 2523-2545.

Wall L, Larocque D, Pierre-Majorique Léger (2008) The early explanatory power of NDVI in crop yield modeling. International Journal of Remote Sensing 29: 2211-2225.

Wiegant CL, Richardson AJ, Kanemasu K (1979) Leaf area index estimates for wheat from Landsat and their implications for evapotranspiration and crop modeling. Agronomy Journal 71: 336-342.

Wong MTF, Asseng S, Zhang H (2006) A flexible approach to managing variability in grain yield and nitrate leaching and within-field to farm scales. Precision Agriculture 7: 405-417.

Yin X, Qi C (1994) Studies on the rice growth calendar model (RICAM) and its application. Acta Agronomica Sinica 20: 339-346.

Zhao CJ, Wang JH, Huang WJ, Zhou QF (2009) Spectral indices sensitively discriminating wheat genotypes of different canopy architectures. Precision Agriculture 11: 557-567.

Zhao DL, Raja Reddyb K, Gopal Kakani BV, Readc JJ, Koti S (2007) Canopy reflectance in cotton for growth assessment and lint yield prediction. Europe Journal of Agronomy 26: 335-344.